IMPROVING DISCRIMINANTS FOR SOURCE IDENTIFICATION

Thorne Lay and Guangwei Fan

University of California, Santa Cruz

Sponsored by Defense Threat Reduction Agency

Contract No. DTRA01-00-C-0211

ABSTRACT

Regional phases in the Tibetan Plateau have anomalous discriminant performance due to low shear wave (Sn, Lg) amplitudes for paths traversing the northern portion of the Plateau. Our investigation of the mechanism responsible for this lack of shear wave energy indicates that strong attenuation in the crust and upper mantle is responsible rather than waveguide blockage effects such as thinning of the crust. This is based on observation of progressive, path-length dependent evolution of the Lg spectra over paths within the Plateau. Anelastic losses, rather than scattering by waveguide disruption, for both Lg and Sn preclude mitigating strategies such as using P/Smax measurements. Thus, improving discrimination for sources in this seismically active region requires improved understanding of the magnitude and spatial variations in shear wave attenuation. In the initial phases of this investigation, reported on last year, we utilized progressive Lg spectral shifts with distance from station WMQ to estimate the attenuation effects for Lg, exploiting the severity of the attenuation to offset the lack of control on source radiation intrinsic to single-station methods. Our preliminary results indicated Lg attenuation with Q_o (1 Hz) values of 85-90 in northern central Tibet, with whole-Tibet path averages of 122-149 for the reliable 0.2-0.5 Hz passband. These values are 2 to 3 times lower than prior published values, most of which omit paths with strong attenuation, suggesting that regional phase attenuation in Tibet has been seriously underestimated, and the resultant problems for discrimination efforts also underestimated. To improve the confidence of our attenuation estimates and to extend the spatial sampling, we have augmented the WMQ observations with observations from LSA, KMI and LZH. These stations provide paths within central Tib*et al*ong with extended sampling of eastern Tibet. As a first-order check on our WMQ observations, we established that all of these stations display strong spectral shifts for the Lg group velocity window as functions of propagation distance. The data from LZH closely parallel those from WMQ, while data for KMI show a slightly lower distance dependence, but still much stronger than observed in China. The LSA observations parallel the trend for WMQ and LZH, but with a baseline shift to lower corner frequencies consistent with having paths entirely within the strongly attenuating Plateau crust. The similarity of the spectral trends results in comparable path averaged attenuation values in the frequency band 0.2-1.0 Hz, but in all cases the signal bandwidth is insufficient to reliably constrain the frequency dependent coefficient of Lg Q. As a result there is some ambiguity in relating our relatively low-frequency results to estimates available for east-central Tibet (about which there is significant controversy, with about a factor of 3 range in reported Q_o values for the same data set). Generally, the data favor a southward increase in Lg Q relative to the very low values found in northernmost Tibet. The latter area spans the region of Cenozoic volcanism in the Plateau along with the region of strong Sn attenuation established in many studies. We have applied a two-station, two-source (close to great-circle) method to estimate Lg Q more accurately on certain paths. Observations at LSA and WMQ have been combined to estimate the Lg Q of northernmost Tibet, resulting in Q_o values of 94 ± 3 and $\eta = 0.29 \pm 0.04$ for the passband 0.2-1.0 Hz. This is very consistent with the results found for WMQ alone. We are currently applying similar analysis to the fundamental mode Rayleigh waves at WMQ and LSA for those events for which focal mechanism estimates are available, in an effort to develop a vertical profile of Q_s in the crust. The two-station method has been applied to WMQ and KMI Lg data as well, providing new constraints on the attenuation in Eastern Tibet. For paths traversing most of the Plateau, we find $Q_o = 183$ for the passband 0.2-1.0 Hz, but as in Central Tibet, there appears to be a strong increase in Q_o toward the south, with the northern region yielding $Q_o = 123$ and the southern region yielding $Q_o = 392$. On the basis of this, we find support for the relatively high Q_o values estimated for east-central Tibet by McNamara *et al*. While efforts to fully map out the Tibetan attenuation structure are continuing, it is clear that the strong regional variations in crustal attenuation will give variable discriminant performance, with paths traversing northern Tibet being particularly prone to anelastic loss of shear wave energy. The effect is so pronounced that path calibration efforts (parametric inversions, kriging, cap-averaging) are not adequate, and one must either calibrate and utilize lower frequency Lg or Sn energy or rely on discriminants other than P/S measures.

OBJECTIVE

Prior work has established that extensive areas of Tibet have very inefficient transmission of *S* waves, for both crustal (*Lg*) and upper mantle (*Sn*) paths. This greatly complicates application of regional seismic discriminants involving *P/S* ratios in the region, and makes Tibet an area of primary concern for seismic monitoring of underground nuclear testing. As part of our multi-year analysis of regional discriminant path corrections in Eurasia, we have been conducting an analysis of *Lg* attenuation within the Tibetan Plateau using the low-frequency passband of 0.2-1.0 Hz to overcome the depletion of high-frequency *Lg* signals within the Plateau. The regional signals for events within the Plateau recorded at stations outside the Plateau often appear rather explosion-like due to the weak *Sn* and *Lg* arrivals, and our work has established that this is most likely due to strong attenuation of shear waves within the crust rather than a structural blockage effect on the Plateau margins. We now believe that there is an extensive region of northern Tibet with 1-Hz Lg attenuation values of 90 –100, which is responsible for the apparent 'blockage' of high-frequency Lg phases observed for paths traversing the northern boundary of the Plateau (Ruzaikin *et al*., 1977, Ni and Barazangi, 1983; Rapine *et al*. 1977; Fan and Lay, 2002).

McNamara *et al*. (1996) analyzed data recorded at 11 broadband stations in eastern central Tibet, finding that high-frequency *Lg* is generated by events within the Plateau, and this energy can propagate to distances of at least 600 km; however, they did not observe the *Lg* phase for even shorter paths traversing western or central Tibet or for events in the Himalayas traveling across the southern margin of the Plateau. For eastern central Tibet, where sufficient high-frequency *Lg* signal-to-noise ratios were observed, a frequency-dependent *Q* function given by $Q(f) = (366\pm37)f^{(0.45\pm0.06)}$ was estimated for the passband (0.5-16 Hz) (McNamara *et al.*, 1996). This is comparable to the estimate of $Q(f)=(448\pm82)f^{(0.426\pm0.157)}$ estimated for 1-6 s *Lg* waves traversing Tibet by Shih *et al.* (1994). This latter value is likely also dominated by eastern Tibet paths, as 'blocked' observations were omitted from the calculation. Similar 1-Hz Q_o value was also estimated to be 340 for events north of LSA using spectral methods by assuming a constant Q_o model (Reese *et al*., 1999). These attenuation values are typical of tectonically active areas and are not low enough to cause rapid extinction of 1-Hz *Lg* over just a few hundred kilometers, as observed for paths traversing the northern margin of Tibet. We believe the explanation is that Q_{Lg} has substantial lateral variations within Tibet. Indeed one might expect this to be the case, for it is true of *Sn* attenuation, which is strongest in northern central Tibet. The possibility of stronger *Lg* attenuation in northern and central Tibet is suggested by the lack of high-frequency *Lg* detections for events to the west of the broadband stations in the data set of McNamara *et al.* (1996). Furthermore, a recent reanalysis of the data set used by McNamara *et al*. (1996) indicates a much lower *Lg Q* in eastern central Tibet, with Q_o = 126 (Xie, 2002). The latter value is almost a factor of 3 lower than the earlier result, which Xie suggested may be due to instabilities in the inversion for source and receiver terms in the formulation by McNamara *et al*. (1996).

Our current work resolves this issue, demonstrating the presence of very strong attenuation in the region of north-central Tibet, an area where other work has demonstrated the presence of partial melt in the crust. We also find average Q_o values for paths traversing the Plateau of about 150, much lower than proposed in earlier work.

RESEARCH ACCOMPLISHED

Work reported on last year utilized regional waveforms recorded at broadband station WMQ, the westernmost station of the Chinese Digital Seismic Network. This station lies just north of the Tarim Basin, about 650 km from the northern boundary of the Tibetan Plateau. While three-component data were obtained, we restricted our analysis to the vertical component seismograms due to the attenuated nature of the *Lg* phases traversing Tibet, which leads to confusion with fundamental mode Love wave energy on the transverse components. We examine energy in the standard *Lg* group velocity window of 3.6 to 3.0 km/s, which precedes short and intermediate period fundamental mode Rayleigh wave energy. We analyzed recordings for 90 earthquakes with magnitudes of $4.4 \le m_b \le 6.4$ that occurred between 1987 and 1999 in the Tibetan Plateau and around its margins. Progressive shifts of frequency content with propagation distance were observed for the WMQ data, leading us to estimate *Lg* attenuation in the 0.2-1.0-Hz frequency band. Given that propagation effects appear to dominate over any plausible source effects, we applied a single-station, multi-event stacking method to obtain the 1-Hz *Lg* attenuation values (Q_o) summarized in Figure 1. The distribution of events enabled whole-Plateau path estimates to be obtained in western, central, and eastern Tibet, along with a more localized estimate for northern-central Tibet. The preferred whole-Plateau estimates, obtained from the passband 0.2-0.5 Hz, involve Q_o values of 122-146, much lower than previously reported within Tibet, with particularly strong attenuation noted for northern central Tibet, where Q_o is about 90.

The concentration of strong attenuation in the northern region of Tibet implies that Q_o in southern central Tibet is actually much higher than the whole-path average, and a value of 316 was determined. It is plausible that there are comparable north-to-south gradients in the western and eastern areas of Tibet; however, the value of 122 found as an average for Eastern Tibet is in close agreement with the value of 126 estimated by Xie (2002), so this need not be the case.

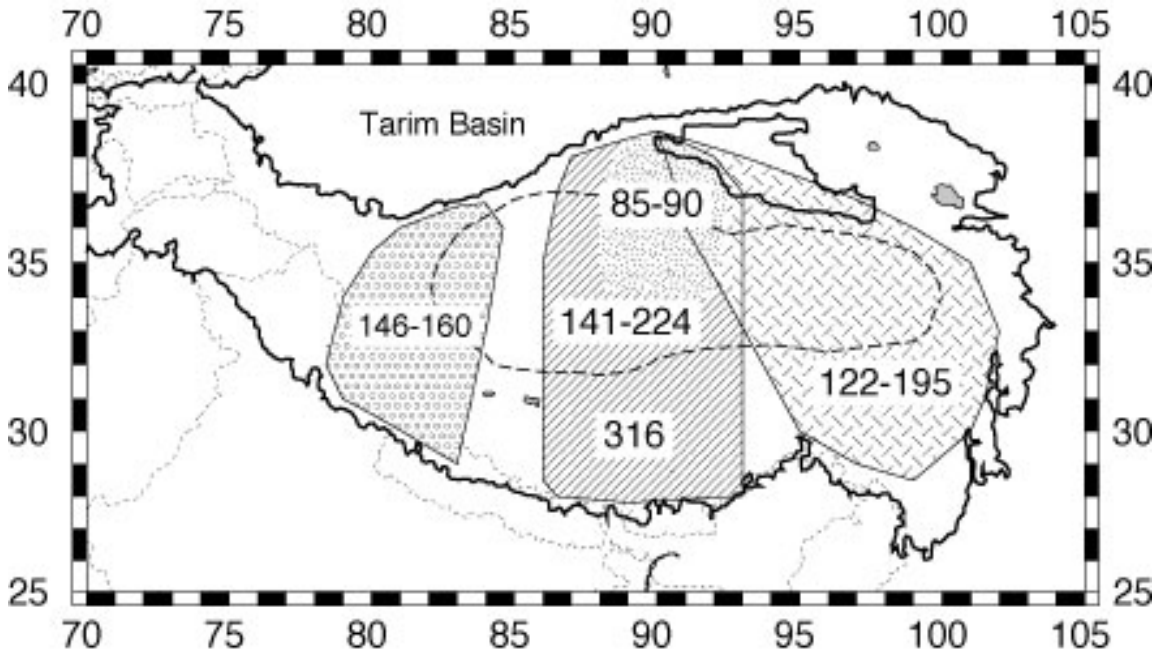

Figure 1. Estimates of *Lg* Q_o variations within the Tibetan Plateau based on single station analysis for data at WMQ. These results were reported on last year, and are based on progressive distance-dependent spectral decay of *Lg* signals for events at the southern edge of each province relative to the northern edge. The first number in each range corresponds to the more reliable spectral range from 0.2-0.5 Hz, with the second number, if given, corresponding to results for the spectral band 0.2-1.0 Hz. The latter band is contaminated by scattered high-frequency *S* energy. In central Tibet, paths traversing the whole Plateau yield overall estimates of 141-224; however, this is resolved to be an average of intense attenuation in the northern third of central Tibet, with much lower attenuation in southern central Tibet. Results are from Fan and Lay (2002).

In this year's continuation of this research, our focus has been on corroborating the results of the single-station analysis for station WMQ, along with extending the spatial coverage using additional broadband stations. We sought all available recordings of Tibetan earthquakes for stations LSA, KMI and LZH. As for WMQ, we began by inspecting systematic range-dependence relative to each station, ignoring source variations. A total of 31 events yielded useful data for LSA, 37 for LZH and 30 for KMI, with the latter two stations yielding extensive coverage of eastern Tibet, while LSA samples the entire Plateau (Figure 2). We estimated an effective 'Lg corner frequency', corresponding to the onset of strong amplitude decrease apparent in all spectra, and regressed the measured values on total path length to each station. As shown in Figure 2 for station LSA, these spectral corners shift very systematically with path length for each station, with distance correlation coefficients of -0.91 for LSA, -0.90 for LZH and -0.95 for KMI, compared to –0.82 for WMQ. We believe that strong attenuation throughout the Plateau is responsible for these spectral shifts with propagation distance that overwhelm any source variations. Tightly fitting regression curves for each station are shown in Figure 3, where it is apparent that the data for WMQ are not anomalous despite all associated paths traversing the northern margin of the Plateau, so any form of crustal structure blockage near the northern boundary is not responsible for this trend.

Given that the attenuation analysis for WMQ suggests average Plateau *Qo* values of around 140, we infer from Figure 3 that similar general results will hold for all 4 stations. However, we note that the WMQ data do appear to

involve averaging of subregions of lower *Q* and subregions of higher *Q*, so mapping out the spatial patterns within the Plateau is essential. The geometry of the event distributions for stations LSA, LZH and KMI is less favorable

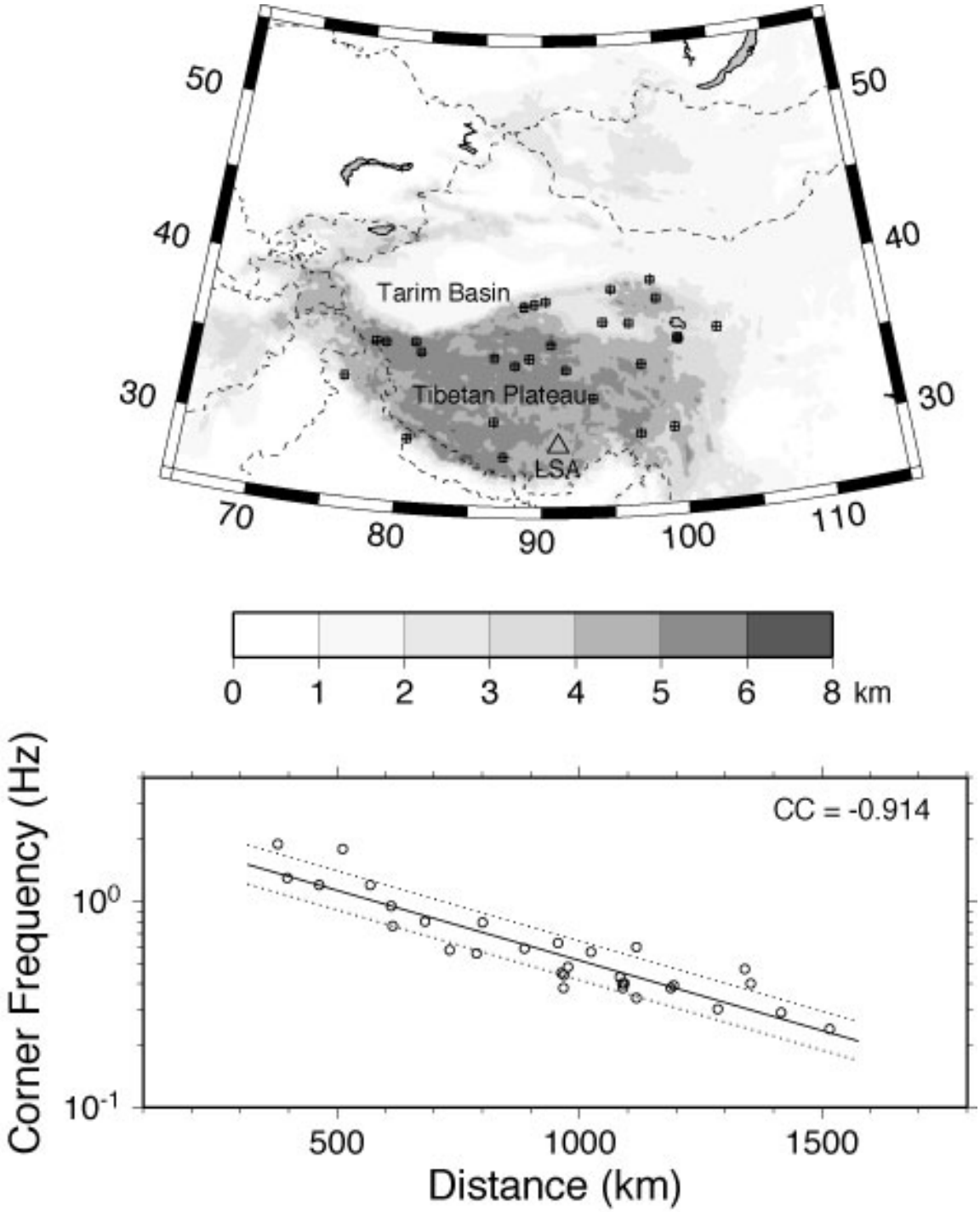

Figure 2. Top: Map showing the location of events yielding useful recordings at station LSA. The associated paths give extensive sampling of the Tibetan Plateau but none of the paths traverse the northern boundary of the Plateau. Bottom: The apparent corner frequency of the *Lg* spectra for each seismogram at LSA is plotted as a function of total path length between source and receiver. The linear correlation coefficient (CC) is indicated at the upper right. The solid line is the result of linear regression, with the dotted lines being ±1 standard deviation about the regression.

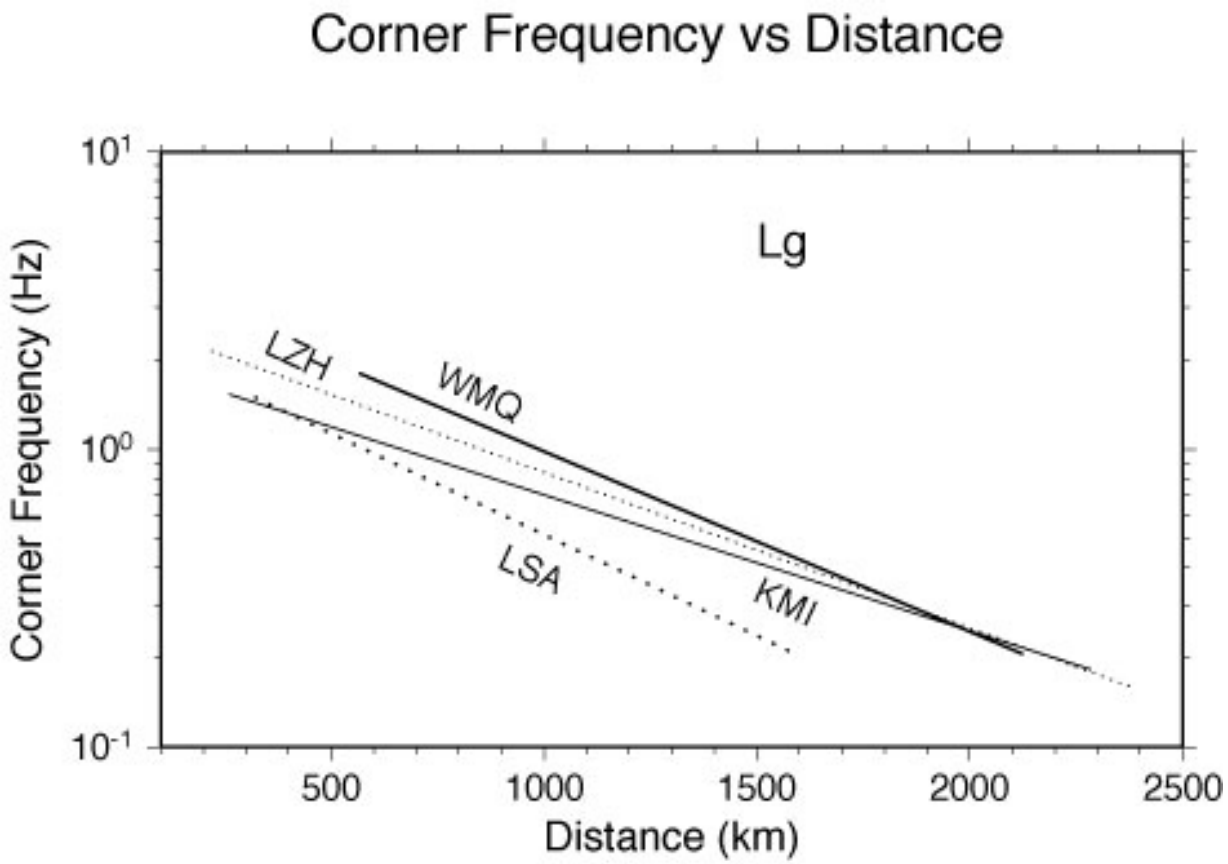

Figure 3. Summary of the regression curves obtained for *Lg* corner frequency versus propagation distance for each of the four stations providing numerous observations of Tibetan events. LSA and WMQ have the most uniform sampling of Tibet, and nearly equivalent regression slopes are found. At a given distance, the entire path to LSA is within the Plateau, while for WMQ, there is at least a 600-km additional path through high *Q* crust north of the Plateau, which accounts for the baseline shift. Paths to LZH and KMI also have portions outside the Plateau, in presumably higher crust as well.

to the single-station spectral stacking approach that was used for WMQ, and we desire to make more precise, spatially resolved estimates of *Lg* attenuation, so we have applied a more restrictive, two-station, two-event method, for the limited geometries in which stations and events are close to a great-circle path. As shown in Figure 4, this is viable using WMQ and LSA, and for WMQ and KMI. The basic approach is that of Chun *et al*. (1987), applied to vertical component *Lg* spectra in the passband 0.2-1.0 Hz. For the geometrical spreading function, we use $d^{-0.5}$, where *d* is the propagation length, as appropriate for spectral observations (Shin and Herrmann, 1987). This procedure explicitly cancels source spectral effects (and azimuthal patterns, to the extent that data are on a great-circle path), and explicitly cancels receiver terms (except to the extent that incoming signals have slightly differing back-azimuths and/or incidence angles). While the assumption of nearly isotropic radiation pattern for *Lg* would allow many more event-station combinations, we feel that it is prudent to restrict this application to nearly great-circle geometries, and this allows us to localize our results to the region between events, given that our stations are always the outer pair of the double combination. Stacking of multiple sets of two-station, two-event spectral estimates further stabilizes the spectral estimates, and reduces any errors associated with slight departures from great-circle geometry. This results in somewhat extended bandwidth at the higher frequency end (between 0.5-1.0 Hz), relative to the single-station spectral stacks for which source corrections were not made.

Our first targeted area was for northern central Tibet where the WMQ results indicated Q_o values near 90. This region is directly along the great-circle between WMQ and LSA (Figure 4), enabling a direct comparison of the

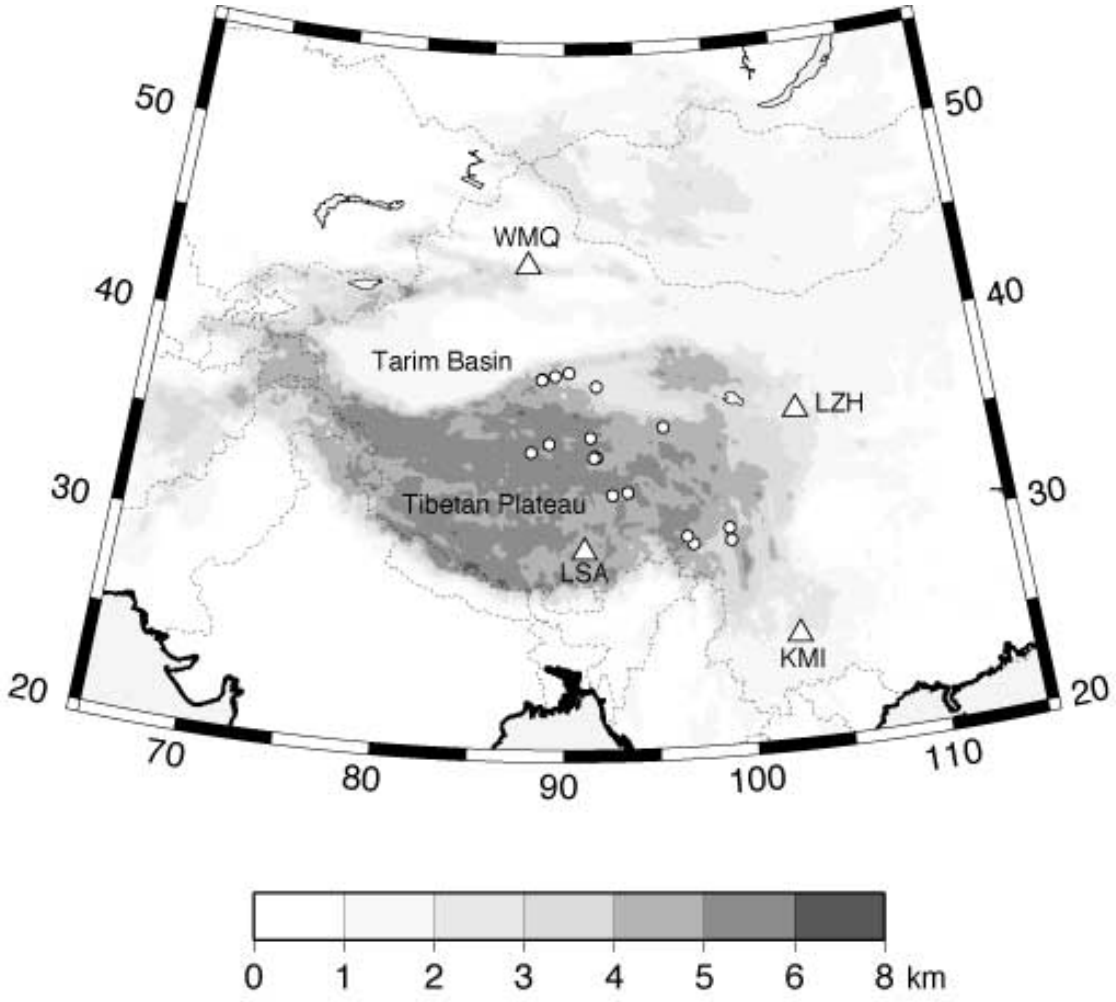

Figure 4. Base map of the study area, showing the topography in Western China and the Tibetan Plateau as well as the location of stations used (triangles) and epicenters of events used for the two-station, two-event applications.

results for one-station, two-event and two-station, two-event methods. Figure 5 shows high-frequency band-passed waveforms for events near the northern boundary of Tibet and about 400 km to the south, as recorded at WMQ and LSA. Note that for the event closer to WMQ, there is clear high-frequency *Lg* energy at WMQ, but no signal above the background noise at LSA, while the opposite is true for the event closer to LSA. This indicates that there is strong depletion of the *Lg* frequency content as a function of increasing distance from LSA, even though the paths never cross the northern boundary of the Tibetan Plateau. This confirms that structural blockage is not responsible, and that a progressive path effect such as attenuation is the explanation for the rapid loss of *Lg* energy in the region. The northern event has a larger *Lg* at WMQ than does the southern event at LSA. This is consistent with a high *Q* path across the Tarim basin to the north, and a moderate attenuation path across southern Tibet to LSA. If the low *Q* region between the two events extended further to the south, the LSA recording from the southern event would be much more depleted in high-frequency *Lg* than is the case. The *Lg/P* ratios indicated in the figure indicate that the primary loss of high-frequency energy is for the shear waves in the *Lg* phase, as high-frequency *P* wave energy does manage to reach stations both to the north and south from each event. The basic strategy of the two-station, two-event method is to compute spectral ratios of the pairs of seismograms for each event (with the more distant station in the numerator) and multiply the spectral ratios, thereby canceling both source and receiver effects. With a correction for geometric spreading over the path length between the sources, the spectra are reduced to a function of the *Lg* attenuation along the path between the sources. The resulting spectra, in the form of the *Lg* attenuation coefficient, are shown in Figure 6, spanning the frequency band 0.2-1.0 Hz. Higher frequency energy in the 1-5 Hz

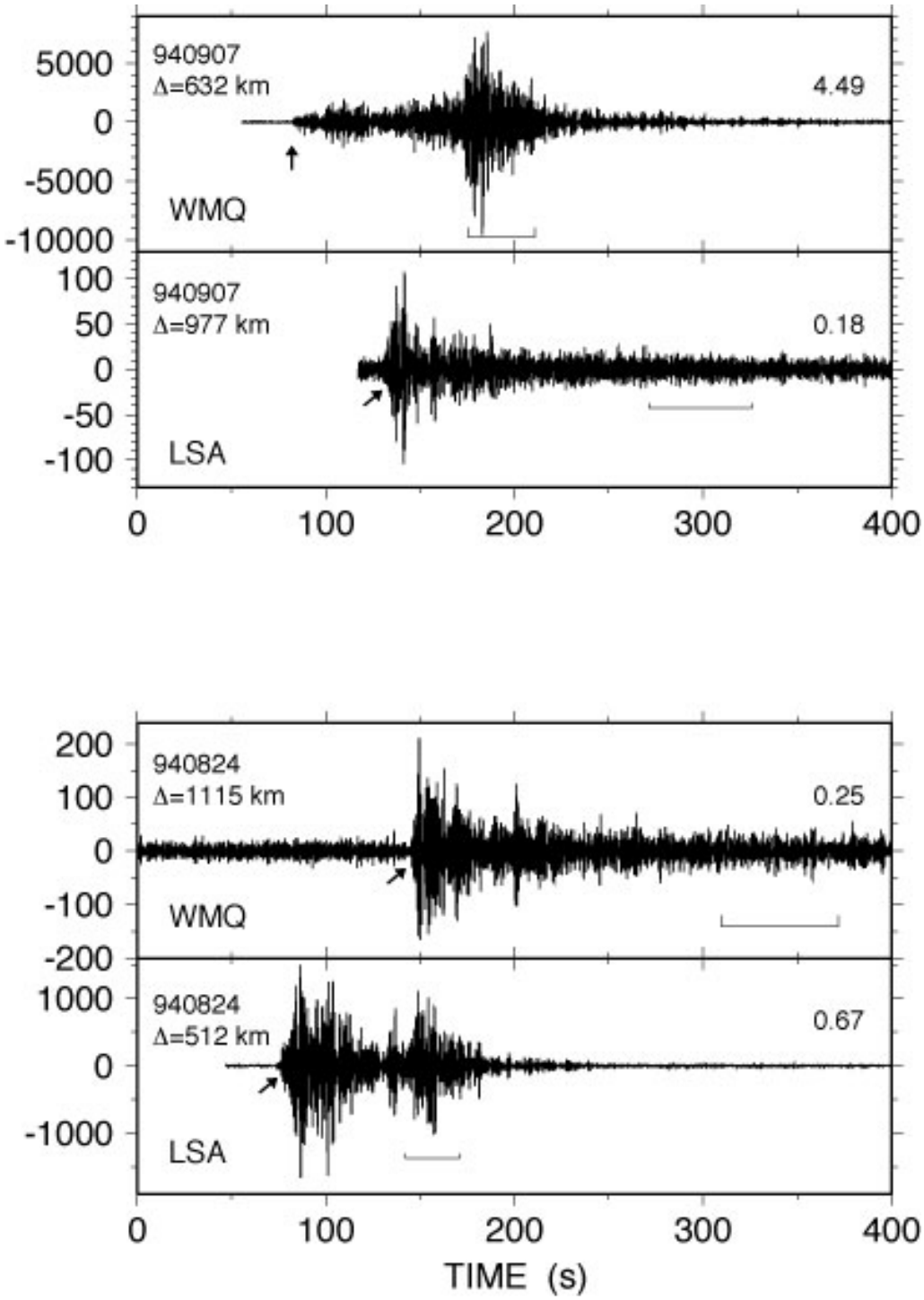

Figure 5. Bandpass (1-5 Hz) filtered seismograms for events recorded by both WMQ and LSA. The upper panels are for an event at the northern edge of Tibet, closer to WMQ. Note the presence of high-frequency energy in the *Lg* window (underlying brackets indicate the *Lg* group velocity window) at WMQ, and its absence at LSA. The amplitude ratio of energy in the Lg window relative to the Pn window is shown on the right (the onset of Pn is marked by the arrowheads). The lower panel is for an event several hundred kilometers to the south, in northern central Tibet. Note the presence of high-frequency *Lg* energy in the LSA recording, but its absence in the WMQ recording. The region between the two sources causes strong attenuation of Lg energy.

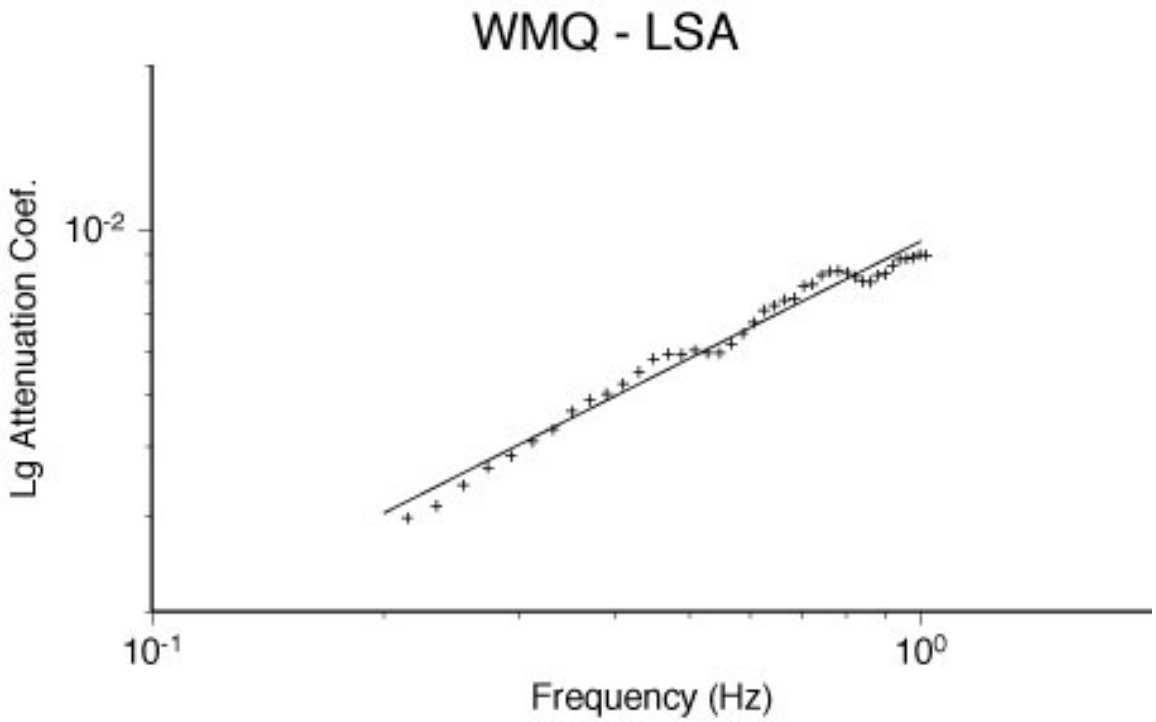

Figure 6. *Lg* attenuation coefficients in the 0.2-1.0 Hz band for the two-station, two-event stacking method WMQ and LSA observations. Twelve event pairs were averaged to give these spectra, so they are very robust. The regression curve is used to estimate Q_o and the frequency dependent parameter η. These spectra give Q_o = 94± 3 and η = 0.29±0.04 for the passband 0.2-1.0 Hz.

band is at the noise level for the more distant observations in each pair (see Figure 5), so we do not extend to higher frequencies. Doing so results in a flattening curve due to contamination from the high-frequency *P* or *Sn* coda seen in the *Lg* window in Figure 5, and that biases the attenuation to higher *Q* estimates. There were 4 events at the north end of this profile and three at the southern end, so a total of 12 spectra processed by the two-event, two-station method were stacked, resulting in the smooth attenuation coefficients shown in Figure 6. The results for velocity spectra in the passband 0.2 to 1.0 Hz are Q_o = 94±3 and η = 0.29±0.04. Processing of displacement spectra gives almost identical results (Q_o = 92±3 and η = 0.28±0.03). The single-station results from WMQ were Q_o = 85±2 (0.2-1.0 Hz) and 90±20 (0.2-0.5 Hz), which is remarkably consistent, given the lack of source corrections. Thus, the LSA-WMQ analysis confirms our result of strong *Lg* attenuation in northern central Tibet.

Corresponding analysis was made for WMQ-KMI combinations sampling eastern Tibet. In this case, the distribution of sources (Figure 4) enables four profiles to be examined, tolerating deviation of up to 30° from the great-circle path. All combinations in eastern Tibet are included in Profile III (named to correspond to the regionalization used in the WMQ analysis). The attenuation coefficient estimates are shown in Figure 7. Table 1

Table 1. The values of *Lg* attenuation in different parts of eastern Tibet.

		Profile III (WMQ)	**Profile III (WMQ-KMI)**	**Profile III (W) (WMQ-KMI)**	**Profile III (NW) (WMQ-KMI)**	**Profile III (SE) (WMQ-KMI)**
0.2-0.5 Hz	Q_o	122±20	119±17	--	--	--
	η	-0.19±0.15	-0.20±0.13	--	--	--
0.2-1.0 Hz	Q_o	195±14	183±13	--	--	--
	η	0.24±0.08	0.22±0.09	--	--	--
0.35-1.0 Hz	Q_o	--	--	199±15	123±3	344±54
	η	--	--	0.28±0.06	0.29±0.05	0.16±0.16

shows the estimated attenuation parameters and compares them to the results from single-station analysis of WMQ. Five event in the north and 4 events in the south were used for Profile III (20 spectral estimates were stacked). The spectra flatten above 0.5 Hz, so the Q_o estimate is very dependent on the frequency range fit, as was found for the WMQ data (Table 1). Given the source cancellation, we have confidence in the 0.2-1.0 Hz results, which give Q_o = 183±13 in eastern Tibet. The western portion of Profile III has higher source density, and whole-Plateau path estimates were made using three northern events and two southern events. Profile III(W) yields a slightly higher Q_o of 199 (Table 1, Figure 7). This portion of the profile is further subdivided into a northwestern section and a southeastern section, with 3x2 and 2x2 event combinations each (the first number indicates number of events at the northern end of each profile and the second number indicates the number of events at the southern end; their product is the total number of spectral estimates that are stacked for each region). Regressions over the 0.35-1.0 Hz range give the results in Table 1, with a strong north-south gradient being present. Again, it appears that very strong attenuation in the northern portion of the Plateau lowers the Plateau-wide averages. The Q_o estimates are shown in map view in Figure 8 for comparison with the results from WMQ analysis in Figure 1. We find it interesting that the relative high Q_o in Profile III (SE) is found in the immediate vicinity of the studies by McNamara *et al*. (1996)

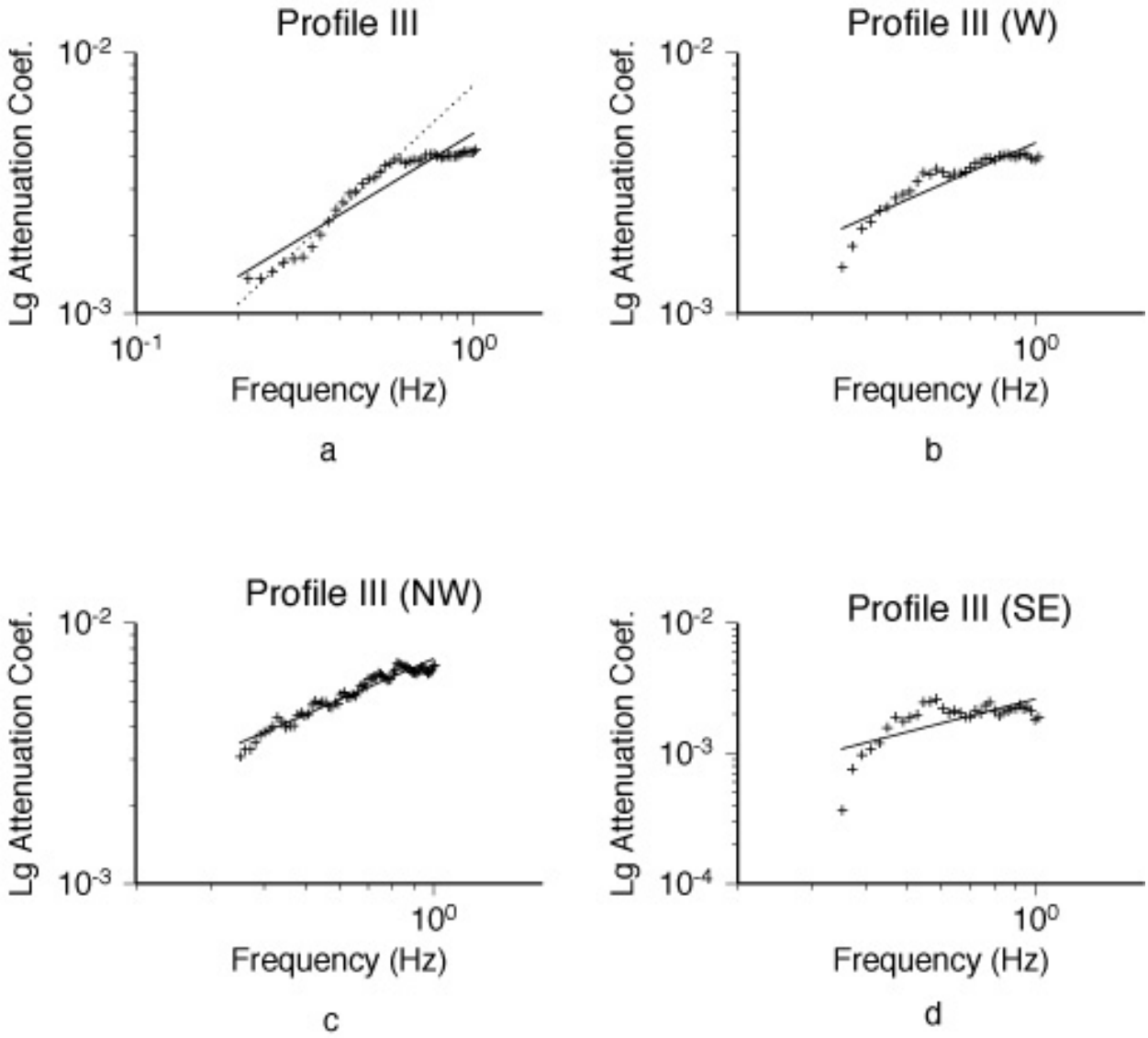

Figure 7. Lg attenuation coefficient estimates from stacking of two-station, two-event combinations for WMQ-KMI recordings. Profile III samples all of eastern Tibet, Profile III (W) is confined to a narrow corridor traversing the entire Plateau in the western portion of Profile III, and Profile III (NW) and (SE) are subdivisions of Profile III (W).

and Xie (2002). Our result is very consistent with the results from McNamara *et al*. (1996), which gave Q_o = 366±37 and η = 0.45±0.06. Our result is also consistent with the work of Reese *et al*. (1999). The results by Xie (2002) warrant further investigation, as the large discrepancy with other results is not clearly explained.

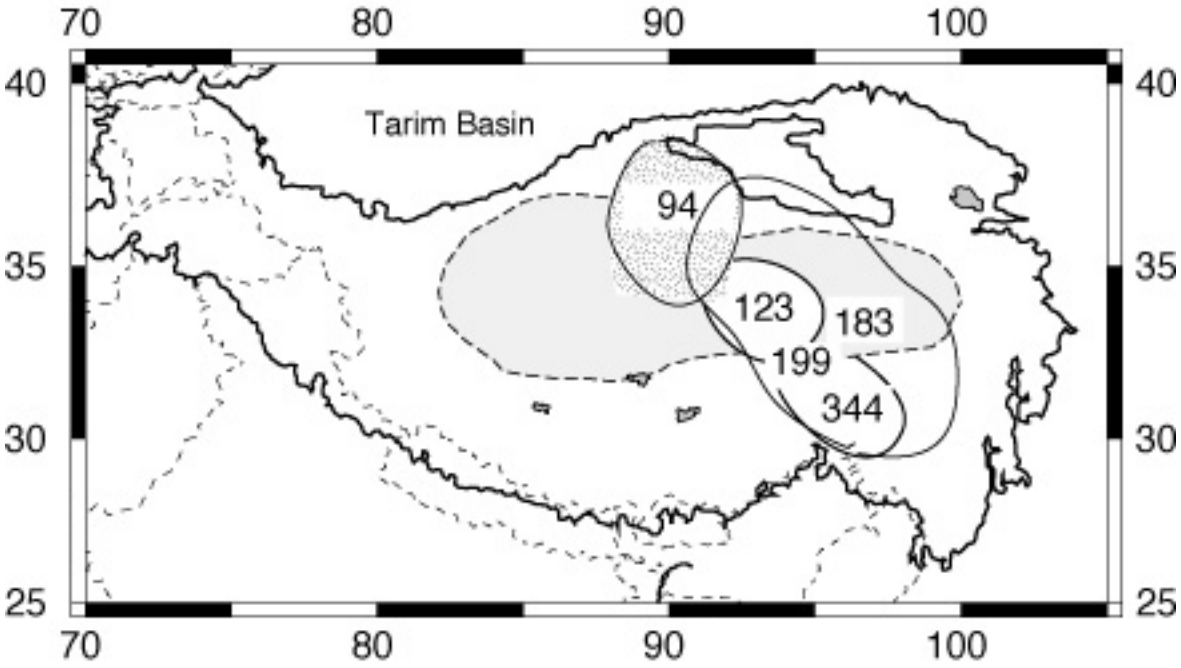

Figure 8. Map of Tibet highlighting regions where 1-Hz *Lg* attenuation coefficient has been estimated by stacking results of two-source/two-station analysis. These results can be compared with Figure 1, obtained by single station analysis of WMQ data. There is a broad region of very low *Q* in northern Tibet with the lowest values in the central region. Average values of *Q* for eastern Tibet are in the 183-218 range, but this is biased low by weighted averaging of the lower *Q* values of the north and the higher *Q* values of the south. The shaded area with dashed line corresponds to the region of inefficient *Sn* propagation in northern Tibet.

CONCLUSIONS AND RECOMMENDATIONS

Tibet has broad regions with some of the strongest *Lg* attenuation values of any continental area [comparably low *Q* values have been reported for the Altiplano in Bolivia (Baumont *et al*., 1999)]. This causes effective extinction of high-frequency *Lg* energy over path lengths of just a few hundred kilometers in northern Tibet. There is substantial spatial variation in attenuation, with the strongest attenuation located in northern central Tibet, the primary region of Cenozoic magmatism within Tibet (Molnar, 1988; Turner *et al*., 1993, 1996; Arnaud *et al*., 1992). Localized regions in southern Tibet appear to have comparably strong *Lg* attenuation over relatively localized regions (Xie, in preparation). Partial melting of the deep crust may be responsible for the strong *Lg* attenuation. There is evidence for a lower crustal low-velocity zone with anomalous Poisson's ratio in northern Tibet (Owens and Zandt, 1997), along with a broad region of inefficient *Sn* propagation (Figure 8; Ni and Barazangi, 1983; McNamara *et al*., 1995) and low Pn velocity (McNamara *et al*., 1997). There is some evidence for partial melt and crustal low-velocity zones north of the Tsangpo suture in southern Tibet (Nelson *et al*., 1996; Kind *et al*., 1996; Cotte *et al*., 1999), so regions of strong *Lg* attenuation in southern Tibet may not have been resolved by our data distribution. Phillips *et al*. (2000) also find north to south gradients in *Lg* attenuation. It is also important to recognize that our results are for the relatively low-frequency band, and due to their narrow-band nature, we cannot place very good results on the frequency variations; thus extrapolation of our values to higher frequency may be erroneous. Nonetheless, we are confident that one cannot invoke uniformly low Q_o values over all of Tibet without violating many observations of high-frequency *Lg* energy at distances where it would be precluded. Systematic mapping of the spatial and

frequency dependence of *Lg* attenuation throughout the Plateau is essential prior to full assessment of the implications for regional discriminant performance in the region.

REFERENCES

Arnaud, N. O., P. Vidal, P. Tapponnier, P. Matte, and M. Deng (1992), The high K_2O volcanism of northwestern Tibet: Geochemistry and tectonic implications, *Earth Planet. Sci. Lett*., **111**, 355-367.

Baumont, D., A. Paul, S. Beck, and G. Zandt (1999). Strong crustal heterogeneity in the Bolivian Altiplano as suggested by attenuation of Lg waves, *J. Geophys. Res*., **104**, 20287-20305.

Chun, K-Y., G. F. West, R. J. Kokoski, and C. Samson (1987), A novel technique for measuring Lg attenuation – Results from Eastern Canada between 1 to 10 Hz, *Bull. Seism. Soc. Am*., **77**, 398-419.

Cotte, N., H. Pedersen, M. Campillo, J. Mars, J.F. Ni, R. Kind, E. Sandvol., and W. Zhao (1999), Determination of the crustal structure in southern Tibet by dispersion and amplitude analysis of Rayleigh waves, *Geophys. J. Int*., **138,** 809-819.

Fan, G., and T. Lay (2002). Characteristics of Lg attenuation in the Tibetan Plateau, *J. Geophys. Res*., in press.

Kind, R., *et al*. (1996), Evidence from earthquake data for a partially molten crustal layer in southern Tibet, *Science*, **274**, 1652-1654.

McNamara, T. J. Owens, and W. R. Walter (1995), Observations of regional phase propagation across the Tibetan Plateau, *J. Geophys. Res.,* **100**, 22215-22229.

McNamara, W. R. Walter, T. J. Owens, and C. J. Ammon (1997), Upper mantle velocity structure beneath the Tibetan Plateau from Pn travel time tomography, *J. Geophys. Res.,* **102**, 493-505.

McNamara, D. E., T. J. Owens, and W. R. Walter (1996), Propagation characteristics of L_g across the Tibetan plateau, *Bull. Seism. Soc. Am*., **86**, 457-469.

Molnar, P. (1988), A review of geophysical constraints on the deep structure of the Tibetan Plateau, the Himalaya and the Karakoram, and their tectonic implications, *Trans. R. Soc*. London, Ser. A, 327, 33-88.

Nelson, K. D., *et al*. (1996), Partially molten middle crust beneath southern Tibet: Synthesis of project INDEPTH results, *Science*, **274**, 1684-1688.

Ni, J. and M. Barazangi (1983), High-frequency seismic wave propagation beneath the Indian Shield, Himalayan Arc, Tibetan Plateau and surrounding regions: high uppermost mantle velocities and efficient S_n propagation beneath Tibet, *Geophys. J. R. astr. Soc.*, **72**, 665-689.

Owens, T. J. and G. Zandt (1997), Implications of crustal property variations for models of Tibetan plateau evolution, *Nature,* **387**, 37-43.

Phillips, W. S., H. E. Hartse, S. R. Taylor, and G. E. Randall (2000), 1 Hz *Lg* Q tomography in central Asia, *Geophys. Res. Let*., **27**, 3425-3428.

Rapine, R. R., J. F. Ni, and T. M. Hearn (1997), Regional wave propagation in China and its surrounding regions, *Bull. Seism. Soc. Am*., **87**, 1622-1636.

Reese, C. C., Rapine, R. R., and J. F. Ni (1999), Lateral variation of Pn and Lg attenuation at the CDSN station LSA, *Bull. Seism. Soc. Am*., **89**, 325-330.

Ruzaikin, A. I., L. Nersesov, V. I. Khalturin, and P. Molnar (1977), Propagation of *Lg* and lateral variations in crustal structure in Asia, *J. Geophys. Res*., **82**, 307-316.

Shih, X. R., K.-Y. Chun, and T. Zhu (1994), Attenuation of 1-6 s *Lg* waves in Eurasia, *J. Geophys. Res*., **99**, 23859-23874.

Shin, T.-C. and R. B. Herrmann (1987), *Lg* attenuation and source studies using 1982 Miramichi data, *Bull. Seism. Soc. Am*., **77**, 384-397.

Turner, S., C. J. Hawkesworth, J. Liu, N. Rogers, S. Kelley, and P. van Calsteren (1993). Timing of Tibetan uplift constrained by analyis of volcanic rocks, *Nature*, **364**, 5053.

Turner, S., N. Arnaud, J. Liu, N. Rogers, C. Hawkesworth, N. Harris, S. Kelley, P. van Calsteren, and W. Deng (1996), Post-collision, shoshonitic volcanism on the Tibetan Plateau: Implications for convective thinning of the lithosphere and the source of ocean island basalts, *J. Petrology*, **37**, 45-71, 1996.

Xie, J. (2002), *Lg* Q in the Eastern Tibetan Plateau, *Bull. Seism. Soc. Am*., **92** 871-876.